

***ANDROGRAPHIS PANICULATA AND CURCUMA
XANTHORRHIZA* EXTRACTS AND ACTIVE
CONSTITUENTS INHIBIT MORPHINE
GLUCURONIDATION**

by

ZULHILMI BIN HUSNI

**Thesis submitted in fulfilment of the requirements for the degree of
Master of Science**

August 2016

ACKNOWLEDGEMENT

All praises and gratitude is due to Allah, the Most Merciful and Compassionate. The completion of this research was not an individual effort as I had supports from many amazing individuals. First of all, I would like to express my sincere gratitude to my project supervisor, Associate Professor Dr. Sabariah Ismail for her encouragement, guidance and support in all the time for research and writing the thesis. The experience that I have gained here in Centre for Drug Research (CDR) was truly invaluable. Her knowledge, comments, and excellent advice have been great values for me. She always been accessible at all the times and made my research is fully guided and rewarding.

I would like to extend my heartfelt gratitude to Professor Dr. Sharif Mahsufi bin Mansor, Director of CDR, for giving me the opportunity to pursue my higher degree in his institution as well as providing me with the facilities critical to the completion of this study.

Not forgetting, a special thanks to the ingenious pedantic academicians including Associate Professor Dr. Mohd Nizam bin Mordi, Associate Professor Dr. Surash Ramanathan, Dr. Lai Choon Sheen, Dr. Siti Rafidah binti Yusof and Dr. Zurina binti Hassan for their profound criticism throughout the progress of this this study.

Last and certainly not the least, a big thanks to the past and present members of CDR graduate students particularly to kak Aziah, kak Mun, kak Yana, kak Fif, kak Shafra, Halim, Atiqah, Izzat, Ahmad, Jimmy and Hema for their sound judgement and indispensable help during the course time of my candidature. Thank you.

Zulhilmi bin Husni

USM, August 2016

TABLE OF CONTENTS

DEDICATION

ACKNOWLEDGEMENT.....	ii
TABLE OF CONTENTS	iii
LIST OF TABLES	xi
LIST OF FIGURES	xii
LIST OF SYMBOLS AND ABBREVIATIONS	xxi
ABSTRAK	xxiii
ABSTRACT.....	xxv

CHAPTER 1 – INTRODUCTION 1

1.1 Background and Highlights	1
1.2 Herbal Medicines.....	4
1.2.1 Medicinal Plant Herbs	4
1.2.2 <i>Andrographis paniculata</i>	6
1.2.2 (a) Taxonomic Hierarchy	7
1.2.2 (b) Phytochemistry of <i>Andrographis paniculata</i>	7
1.2.2 (c) Pharmacological Properties of <i>Andrographis paniculata</i>	8
1.2.3 <i>Curcuma xanthorrhiza</i>	9
1.2.3 (a) Taxonomic Hierarchy	10
1.2.3 (b) Phytochemistry of <i>Curcuma xanthorrhiza</i>	10
1.2.3 (c) Pharmacological Properties of <i>Curcuma xanthorrhiza</i>	11
1.3 Drug Metabolism.....	12
1.3.1 Drug Metabolizing Enzymes.....	12
1.3.2 UGT Enzymes	13
1.3.3 Latency of Microsomal UGTs.....	14
1.3.4 <i>In-vitro</i> Model	15

1.3.5	Drug Interaction through Glucuronidation	16
1.4	Enzyme Kinetics.....	17
1.4.1	Michaelis-Menten Kinetics.....	17
1.4.2	Initial Rate of Reaction.....	21
1.4.3	Linear transformation of Michaelis-Menten Kinetics	22
1.4.4	Enzyme Inhibition	23
1.4.4 (a)	Competitive-Type Inhibition	24
1.4.4 (b)	Uncompetitive-Type Inhibition	28
1.4.4 (c)	Mixed-Type Inhibition.....	31
1.4.4 (d)	Noncompetitive-Type Inhibition	33
1.4.5	Inhibition Constant	35
1.4.6	[i]/K _i Ratio.....	38
1.5	Morphine	40
1.5.1	UGTs that Metabolize Morphine.....	41
1.5.2	Morphine as a Substrate in UGT2B7 Glucuronidation Activity	41
1.5.3	Unexpected Lipophilicity of Morphine-6-glucuronide	42
1.5.4	UGT2B7 Endogenous Inhibitors: Unsaturated Long Chain Fatty Acids	43
1.6	Instrumentation	44
1.6.1	High Performance Liquid Chromatography (HPLC)	44
1.6.2	HPLC Method Validation.....	44
1.6.2 (a)	Selectivity	45
1.6.2 (b)	Calibration Curves	45
1.6.2 (c)	Quality Controls.....	45
1.6.2 (d)	Limit of Detection	46
1.6.2 (e)	Limit of Quantification	46
1.6.2 (f)	Accuracy	47
1.6.2 (g)	Precision	47
1.6.2 (h)	Recovery from Matrix Effect	47

1.7	Problem Statement.....	48
1.8	Research Objectives.....	48
1.9	Research Design	49
CHAPTER 2 – METHODOLOGY		50
2.1	Chemicals	50
2.2	Preparation of Herbal Extracts and Its Phytoconstituents	50
2.2.1	Aqueous Extract Preparation	51
2.2.2	Ethanollic Extract Preparation.....	51
2.2.3	Phytoconstituents.....	51
2.3	Source of Enzymes	51
2.3.1	Recombinant Protein UGT2B7	51
2.3.2	Human Liver Microsomes	52
2.4	Instrumentation.....	52
2.4.1	HPLC Equipment	52
2.4.2	HPLC Method	52
2.4.3	HPLC Method Validation.....	53
2.4.3 (a)	Selectivity	53
2.4.3 (b)	Calibration curves.....	53
2.4.3 (c)	Quality Controls.....	53
2.4.3 (d)	Limit of Detection and Quantification.....	54
2.4.3 (e)	Accuracy and Precision	54
2.4.3 (f)	Recovery from Matrix Effects.....	54
2.5	Other Equipment.....	54
2.6	Preliminary Experiment – Optimization of Reaction Condition	54
2.6.1	Morphine Glucuronidation Assay	55
2.6.2	Alamethicin Content Optimization.....	57
2.6.3	BSA Content Optimization.....	57

2.6.4	Initial Rate of Reaction.....	58
2.6.5	K_m and V_{max}	58
2.6.6	Reduction of Michaelis-Menten Constant, K_m in Presence of BSA.....	58
2.6.7	Inhibition of Morphine Glucuronidation by Known Inhibitor	58
2.7	Inhibition Assays	59
2.7.1	Preliminary Inhibition Studies.....	59
2.7.2	Dose-Response Inhibition Assay (Measurement of IC_{50}).....	59
2.7.3	Determination of Type of Inhibition	60
2.7.4	Determination of Inhibition Constant.....	60
2.8	Data Analysis.....	61
CHAPTER 3 – RESULTS.....		63
3.1	Validation of HPLC Method for Morphine and its Glucuronides	63
3.1.1	Selectivity	63
3.1.2	Calibration Curves.....	65
3.1.3	Limit of Detection and Quantification.....	66
3.1.4	Accuracy and Precision	67
3.1.5	Recovery from Matrix Effect	68
3.2	Optimization of Morphine Glucuronidation Assay in Recombinant UGT2B7	68
3.2.1	Alamethicin Content Optimization in Recombinant UGT2B7	69
3.2.2	BSA Content Optimization in Recombinant UGT2B7	70
3.2.3	Determination of Initial Rate Condition in Recombinant UGT2B7.....	71
3.2.4	Determination of V_{max} and K_m Values in Recombinant UGT2B7.....	72
3.3	Optimization of Morphine Glucuronidation Assay in Human Liver Microsomes	73
3.3.1	Alamethicin Content Optimization in Human Liver Microsomes.....	73
3.3.2	BSA Content Optimization in Human Liver Microsomes	74
3.3.3	Determination of Initial Rate Condition in Human Liver Microsomes	75
3.3.4	Determination of V_{max} and K_m Values in Human Liver Microsomes.....	76

3.4	Reduction of Michaelis-Menten Constant, Km in Presence of BSA.....	76
3.5	Inhibition of Morphine Glucuronidation by Known Inhibitor.....	78
3.6	Preliminary Inhibition Studies in Recombinant UGT2B7.....	81
3.6.1	Preliminary Inhibition of <i>Andrographis paniculata</i> Ethanolic Extract in Recombinant UGT2B7.....	81
3.6.2	Preliminary Inhibition of <i>Andrographis paniculata</i> Aqueous Extract in Recombinant UGT2B7.....	82
3.6.3	Preliminary Inhibition of Andrographolide in Recombinant UGT2B7.....	83
3.6.4	Preliminary Inhibition of Neoandrographolide in Recombinant UGT2B7.....	84
3.6.5	Preliminary Inhibition of <i>Curcuma xanthorrhiza</i> Ethanolic Extract in Recombinant UGT2B7.....	85
3.6.6	Preliminary Inhibition of <i>Curcuma xanthorrhiza</i> Aqueous Extract in Recombinant UGT2B7.....	86
3.6.7	Preliminary Inhibition of Xanthorrhizol in Recombinant UGT2B7.....	87
3.6.8	Preliminary Inhibition of Curcumin in Recombinant UGT2B7.....	88
3.7	Preliminary Inhibition Studies in Human Liver Microsomes.....	89
3.7.1	Preliminary Inhibition of <i>Andrographis paniculata</i> Ethanolic Extract in Human Liver Microsomes.....	89
3.7.2	Preliminary Inhibition of <i>Andrographis paniculata</i> Aqueous Extract in Human Liver Microsomes.....	90
3.7.3	Preliminary Inhibition of Andrographolide in Human Liver Microsomes.....	91
3.7.4	Preliminary Inhibition of Neoandrographolide in Human Liver Microsomes.....	92
3.7.5	Preliminary Inhibition of <i>Curcuma xanthorrhiza</i> Ethanolic Extract in Human Liver Microsomes.....	93
3.7.6	Preliminary Inhibition of <i>Curcuma xanthorrhiza</i> Aqueous Extract in Human Liver Microsomes.....	94
3.7.7	Preliminary Inhibition of Xanthorrhizol in Human Liver Microsomes.....	95
3.7.8	Preliminary Inhibition of Curcumin in Human Liver Microsomes.....	96

3.8	Determination of IC ₅₀ in Recombinant UGT2B7	97
3.8.1	Determination of IC ₅₀ of <i>Andrographis paniculata</i> Ethanolic Extract in Recombinant UGT2B7	98
3.8.2	Determination of IC ₅₀ of <i>Andrographis paniculata</i> Aqueous Extract in Recombinant UGT2B7	99
3.8.3	Determination of IC ₅₀ of Andrographolide in Recombinant UGT2B7	100
3.8.4	Determination of IC ₅₀ of <i>Curcuma xanthorrhiza</i> Ethanolic Extract in Recombinant UGT2B7	101
3.8.5	Determination of IC ₅₀ of <i>Curcuma xanthorrhiza</i> Aqueous Extract in Recombinant UGT2B7	102
3.8.6	Determination of IC ₅₀ of Xanthorrhizol in Recombinant UGT2B7	103
3.9	Determination of IC ₅₀ in Human Liver Microsomes	104
3.9.1	Determination of IC ₅₀ of <i>Andrographis paniculata</i> Ethanolic Extract in Human Liver Microsomes.....	105
3.9.2	Determination of IC ₅₀ of <i>Andrographis paniculata</i> Aqueous Extract in Human Liver Microsomes.....	106
3.9.3	Determination of IC ₅₀ of Andrographolide in Human Liver Microsomes	107
3.9.4	Determination of IC ₅₀ of <i>Curcuma xanthorrhiza</i> Ethanolic Extract in Human Liver Microsomes	108
3.9.5	Determination of IC ₅₀ of <i>Curcuma xanthorrhiza</i> Aqueous Extract in Human Liver Microsomes	109
3.9.6	Determination of IC ₅₀ of Xanthorrhizol in Human Liver Microsomes	110
3.10	Determination of Type of Inhibition in Recombinant UGT2B7	111
3.10.1	Lineweaver-Burk Plot of <i>Andrographis paniculata</i> Ethanolic Extract in Recombinant UGT2B7	112
3.10.2	Lineweaver-Burk Plot of Andrographolide in Recombinant UGT2B7	113
3.10.3	Lineweaver-Burk Plot of <i>Curcuma xanthorrhiza</i> Ethanolic Extract in Recombinant UGT2B7	114

3.10.4	Lineweaver-Burk Plot of Xanthorrhizol in Recombinant UGT2B7.....	115
3.11	Determination of Type of Inhibition in Human Liver Microsomes	116
3.11.1	Lineweaver-Burk Plot of <i>Andrographis paniculata</i> Ethanolic Extract in Human Liver Microsomes.....	117
3.11.2	Lineweaver-Burk Plot of Andrographolide in Human Liver Microsomes.....	118
3.11.3	Lineweaver-Burk Plot of <i>Curcuma xanthorrhiza</i> Ethanolic Extract in Human Liver Microsomes	119
3.11.4	Lineweaver-Burk Plot of Xanthorrhizol in Human Liver Microsomes.....	120
3.12	Determination of Inhibition Constant in Recombinant UGT2B7.....	121
3.12.1	Dixon Plot of <i>Andrographis paniculata</i> Ethanolic Extract in Recombinant UGT2B7	122
3.12.2	Cornish-Bowden Plot of <i>Andrographis paniculata</i> Ethanolic Extract in Recombinant UGT2B7.....	123
3.12.3	Dixon Plot of Andrographolide in Recombinant UGT2B7.....	124
3.12.4	Cornish-Bowden Plot of Andrographolide in Recombinant UGT2B7.....	125
3.12.5	Dixon Plot of <i>Curcuma xanthorrhiza</i> Ethanolic Extract in Recombinant UGT2B7	126
3.12.6	Cornish-Bowden Plot of <i>Curcuma xanthorrhiza</i> Ethanolic Extract in Recombinant UGT2B7	127
3.12.7	Dixon Plot of Xanthorrhizol in Recombinant UGT2B7.....	128
3.12.8	Cornish-Bowden Plot of Xanthorrhizol in Recombinant UGT2B7.....	129
3.13	Determination of Inhibition Constant in Human Liver Microsomes.....	130
3.13.1	Dixon Plot of <i>Andrographis paniculata</i> Ethanolic Extract in Human Liver Microsomes	131
3.13.2	Cornish-Bowden Plot of <i>Andrographis paniculata</i> Ethanolic Extract in Human Liver Microsomes.....	132
3.13.3	Dixon Plot of Andrographolide in Human Liver Microsomes	133
3.13.4	Cornish-Bowden Plot of Andrographolide in Human Liver Microsomes.....	134

3.13.5 Dixon Plot of <i>Curcuma xanthorrhiza</i> Ethanolic Extract in Human Liver Microsomes	135
3.13.6 Cornish-Bowden Plot of <i>Curcuma xanthorrhiza</i> Ethanolic Extract in Human Liver Microsomes	136
3.13.7 Dixon Plot of Xanthorrhizol in Human Liver Microsomes	137
3.13.8 Cornish-Bowden Plot of Xanthorrhizol in Human Liver Microsomes.....	138
3.14 Result Summaries	139
3.14.1 Inhibitory Effects of <i>Andrographis paniculata</i> and Its Phytoconstituents on Morphine Glucuronidation in Recombinant UGT2B7	139
3.14.2 Inhibitory Effects of <i>Andrographis paniculata</i> and Its Phytoconstituents on Morphine Glucuronidation in Human Liver Microsomes	140
3.14.3 Inhibitory Effects of <i>Curcuma xanthorrhiza</i> and Its Phytoconstituents on Morphine Glucuronidation in Recombinant UGT2B7.....	141
3.14.4 Inhibitory Effects of <i>Curcuma xanthorrhiza</i> and Its Phytoconstituents on Morphine Glucuronidation in Human Liver Microsomes.....	142
CHAPTER 4 – DISCUSSION.....	143
CHAPTER 5 – CONCLUSION.....	151
5.1 Conclusions	151
5.2 Research Limitations	152
5.3 Future Directions	153
REFERENCES.....	154
APPENDIX.....	160

LIST OF TABLES

	Page
1.1 Recommendation of clinical test for enzyme inhibition study of investigational drug that inhibit the metabolism of other co-administered drugs.	39
2.1 The portion of enzyme incubation components in morphine glucuronidation assay.	55
2.2 Choice of concentration range of plant extracts and their phytoconstituents on measurement of IC ₅₀ through dose-response inhibition assay.	60
2.3 Choice of concentration range of substrate (morphine) and potential inhibitors on measurement of inhibition constant (K _i).	61
3.1 Accuracy and precision of morphine-3-glucuronide calibration standard.	67
3.2 Accuracy and precision of morphine-6-glucuronide calibration standard.	67
3.3 Recovery of calibrators from matrix effect.	68
3.4 Inhibitory effect of <i>Andrographis paniculata</i> and its phytoconstituents on the formation rate of morphine glucuronides in recombinant UGT2B7.	133
3.5 Inhibitory effect of <i>Andrographis paniculata</i> and its phytoconstituents on the formation rate of morphine glucuronides in human liver microsomes.	134
3.6 Inhibitory effect of <i>Curcuma xanthorrhiza</i> and its phytoconstituents on the formation rate of morphine glucuronides in recombinant UGT2B7.	135
3.7 Inhibitory effect of <i>Curcuma xanthorrhiza</i> and its phytoconstituents on the formation rate of morphine glucuronides in human liver microsomes.	136

LIST OF FIGURES

	Page
1.1 Morphology of <i>Andrographis paniculata</i> plant parts.	6
1.2 Selected phytoconstituents of <i>Andrographis paniculata</i> to be used in the study.	8
1.3 Morphology of <i>Curcuma xanthorrhiza</i> plant parts.	9
1.4 Selected phytoconstituents of <i>Curcuma xanthorrhiza</i> to be used in the study	11
1.5 Glucuronic acid conjugation of a substrate catalyzed by UGT enzymes producing a highly soluble metabolite.	13
1.6 Schematic representation of UGT protein (UGT1A1) within the luminal wall of endoplasmic reticulum (ER).	14
1.7 Schematic of alamethicin pores in membrane bilayer.	15
1.8 Change in concentration over time of enzyme [E], substrate [S], enzyme-substrate complex [ES] and product [P].	18
1.9 Representative hyperbolic plot of a reaction following Michaelis-Menten Kinetics.	21
1.10 Double reciprocal plot of reaction velocity, v as a function of substrate concentration, [S] yielding a linearized Michaelis-Menten relationship.	23
1.11 Lineweaver-Burk plot of the rate of substrate turnover by an enzyme in the presence of a competitive inhibitor at varying inhibitor concentration.	28
1.12 Lineweaver-Burk plot of the rate of substrate turnover by an enzyme in the presence of an uncompetitive inhibitor at varying inhibitor concentration.	31

1.13	Lineweaver-Burk plot of the rate of substrate turnover by an enzyme in the presence of inhibitor that having both natures of competitive and uncompetitive.	33
1.14	Lineweaver-Burk plot of the rate of substrate turnover by an enzyme in the presence of a non-competitive inhibitor at varying inhibitor concentration.	35
1.15	Determination of enzyme inhibition constants.	37
1.16	Capsule of <i>Papaver somniferum</i> showing latex (opium) exuding out from incision of the green seed pod.	40
1.17	Friedrich Wilhelm Adam Sertürner.	41
1.18	3-Dimensional protein structure of UDP glucuronosyltransferase 2 family, polypeptide B7 (UGT2B7).	42
1.19	Glucuronidation of morphine catalyzed by UGT2B7 yielding morphine-3-glucuronide and morphine-6-glucuronide as metabolites.	42
1.20	Experimental design on the effect of selected Malaysian medicinal plant herbs on morphine glucuronidation	49
3.1	HPLC chromatogram of 100 pmol of morphine-3-glucuronide and 10 pmol of morphine-6-glucuronide mixed standards in distilled water.	63
3.2	HPLC chromatogram of incubation assay in absence of UDPGA and inhibitor incubated at optimized condition.	64
3.3	HPLC chromatogram of incubation assay in absence of inhibitor at optimized condition (10% product formation).	64
3.4	Calibration curves of morphine metabolites at various ranges.	65
3.5	Optimization of alamethicin content in incubation with recombinant UGT2B7 enzyme.	69

3.6	Optimization of BSA content in incubation with recombinant UGT2B7 enzyme.	70
3.7	Determination of initial rate conditions at formation of product not more than 10% for recombinant UGT2B7 model.	71
3.8	Michaelis-Menten plot for morphine glucuronidation catalysed by recombinant UGT2B7 enzyme.	72
3.9	Optimization of alamethicin content in incubation with human liver microsomes.	73
3.10	Optimization of BSA content in incubation with human liver microsomes.	74
3.11	Determination of initial rate condition at formation of product not more than 10% for human liver microsomal model.	75
3.12	Michaelis-Menten plot for morphine glucuronidation catalysed by human liver microsomes.	76
3.13	Reduction of Km value of morphine-3-glucuronidation in presence of BSA.	77
3.14	Reduction of Km value of morphine-6-glucuronidation in presence of BSA.	77
3.15	Lineweaver-Burk plots of the Inhibition of Morphine glucuronidation by ketamine for (A) morphine-3-glucuronide and (B) morphine-6-glucuronide.	78
3.16	Dixon plots of the Inhibition of (A) morphine-3-glucuronide and (B) morphine-6-glucuronide formations by ketamine.	79
3.17	Cornish-Bowden plots of the Inhibition of (A) morphine-3-glucuronide and (B) morphine-6-glucuronide formations by ketamine in human liver microsomes.	80
3.18	Screening of concentration range of <i>Andrographis paniculata</i> ethanolic extract for IC ₅₀ measurement in recombinant UGT2B7.	81

3.19	Screening of concentration range of <i>Andrographis paniculata</i> aqueous extract for IC ₅₀ measurement in recombinant UGT2B7.	82
3.20	Screening of concentration range of andrographolide for IC ₅₀ measurement in recombinant UGT2B7.	83
3.21	Screening of concentration range of neoandrographolide for IC ₅₀ measurement in recombinant UGT2B7.	84
3.22	Screening of concentration range of <i>Curcuma xanthorrhiza</i> ethanolic extract for IC ₅₀ measurement in recombinant UGT2B7.	85
3.23	Screening of concentration range of <i>Curcuma xanthorrhiza</i> aqueous extract for IC ₅₀ measurement in recombinant UGT2B7.	86
3.24	Screening of concentration range of xanthorrhizol for IC ₅₀ measurement in recombinant UGT2B7.	87
3.25	Screening of concentration range of curcumin for IC ₅₀ measurement in recombinant UGT2B7.	88
3.26	Screening of concentration range of <i>Andrographis paniculata</i> ethanolic extract for IC ₅₀ measurement in human liver microsomes.	89
3.27	Screening of concentration range of <i>Andrographis paniculata</i> aqueous extract for IC ₅₀ measurement in human liver microsomes.	90
3.28	Screening of concentration range of andrographolide for IC ₅₀ measurement in human liver microsomes.	91
3.29	Screening of concentration range of neoandrographolide for IC ₅₀ measurement in human liver microsomes.	92
3.30	Screening of concentration range of <i>Curcuma xanthorrhiza</i> ethanolic extract for IC ₅₀ measurement in human liver microsomes.	93

3.31	Screening of concentration range of <i>Curcuma xanthorrhiza</i> aqueous extract for IC ₅₀ measurement in human liver microsomes.	94
3.32	Screening of concentration range of xanthorrhizol for IC ₅₀ measurement in human liver microsomes.	95
3.33	Screening of concentration range of curcumin for IC ₅₀ measurement in human liver microsomes.	96
3.34	IC ₅₀ plots for the inhibitory effect of <i>Andrographis paniculata</i> ethanolic extract on the formation rate of (A) morphine-3-glucuronide and (B) morphine-6-glucuronide in recombinant UGT2B7.	97
3.35	IC ₅₀ plots for the inhibitory effect of <i>Andrographis paniculata</i> aqueous extract on the formation rate of (A) morphine-3-glucuronide and (B) morphine-6-glucuronide in recombinant UGT2B7.	98
3.36	IC ₅₀ plots for the inhibitory effect of andrographolide on the formation rate of (A) morphine-3-glucuronide and (B) morphine-6-glucuronide in recombinant UGT2B7.	99
3.37	IC ₅₀ plots for the inhibitory effect of <i>Curcuma xanthorrhiza</i> ethanolic extract on the formation rate of (A) morphine-3-glucuronide and (B) morphine-6-glucuronide in recombinant UGT2B7.	100
3.38	IC ₅₀ plots for the inhibitory effect of <i>Curcuma xanthorrhiza</i> aqueous extract on the formation rate of (A) morphine-3-glucuronide and (B) morphine-6-glucuronide in recombinant UGT2B7.	101
3.39	IC ₅₀ plots for the inhibitory effect of xanthorrhizol on the formation rate of (A) morphine-3-glucuronide and (B) morphine-6-glucuronide in recombinant UGT2B7.	102
3.40	IC ₅₀ plots for the inhibitory effect of <i>Andrographis paniculata</i> ethanolic extract on the formation rate of (A) morphine-3-glucuronide and (B) morphine-6-glucuronide in human liver microsomes.	103

3.41	IC ₅₀ plots for the inhibitory effect of <i>Andrographis paniculata</i> aqueous extract on the formation rate of (A) morphine-3-glucuronide and (B) morphine-6-glucuronide in human liver microsomes.	104
3.42	IC ₅₀ plots for the inhibitory effect of andrographolide on the formation rate of (A) morphine-3-glucuronide and (B) morphine-6-glucuronide in human liver microsomes.	105
3.43	IC ₅₀ plots for the inhibitory effect of <i>Curcuma xanthorrhiza</i> ethanolic extract on the formation rate of (A) morphine-3-glucuronide and (B) morphine-6-glucuronide in human liver microsomes.	106
3.44	IC ₅₀ plots for the inhibitory effect of <i>Curcuma xanthorrhiza</i> aqueous extract on the formation rate of (A) morphine-3-glucuronide and (B) morphine-6-glucuronide in human liver microsomes.	107
3.45	IC ₅₀ plots for the inhibitory effect of xanthorrhizol on the formation rate of (A) morphine-3-glucuronide and (B) morphine-6-glucuronide in human liver microsomes.	108
3.46	Lineweaver-Burk plots of the inhibitory effect of <i>Andrographis paniculata</i> ethanolic extract on the formation rate of (A) morphine-3-glucuronide and (B) morphine-6-glucuronide in recombinant UGT2B7.	109
3.47	Lineweaver-Burk plots of the inhibitory effect of andrographolide on the formation rate of (A) morphine-3-glucuronide and (B) morphine-6-glucuronide in recombinant UGT2B7.	110
3.48	Lineweaver-Burk plots of the inhibitory effect of <i>Curcuma xanthorrhiza</i> ethanolic extract on the formation rate of (A) morphine-3-glucuronide and (B) morphine-6-glucuronide in recombinant UGT2B7.	111
3.49	Lineweaver-Burk plots of the inhibitory effect of xanthorrhizol on the formation rate of (A) morphine-3-glucuronide and (B) morphine-6-glucuronide in recombinant UGT2B7.	112

3.50	Lineweaver-Burk plots of the inhibitory effect of <i>Andrographis paniculata</i> ethanolic extract on the formation rate of (A) morphine-3-glucuronides and (B) morphine-6-glucuronide in human liver microsomes.	113
3.51	Lineweaver-Burk plots of the inhibitory effect of andrographolide on the formation rate of (A) morphine-3-glucuronides and (B) morphine-6-glucuronide in human liver microsomes.	114
3.52	Lineweaver-Burk plots of the inhibitory effect of <i>Curcuma xanthorrhiza</i> ethanolic extract on the formation rate of (A) morphine-3-glucuronides and (B) morphine-6-glucuronide in human liver microsomes.	115
3.53	Lineweaver-Burk plots of the inhibitory effect of xanthorrhizol on the formation rate of (A) morphine-3-glucuronides and (B) morphine-6-glucuronide in human liver microsomes.	116
3.54	Dixon plots of the inhibitory effect of <i>Andrographis paniculata</i> ethanolic extract on the formation rate of (A) morphine-glucuronide and (B) morphine-6-glucuronide in recombinant UGT2B7.	117
3.55	Cornish-Bowden plots of the inhibitory effect of <i>Andrographis paniculata</i> ethanolic extract on the formation rate of (A) morphine-glucuronide and (B) morphine-6-glucuronide in recombinant UGT2B7.	118
3.56	Dixon plots of the inhibitory effect of andrographolide on the formation rate of (A) morphine-3-glucuronide and (B) morphine-6-glucuronide in recombinant UGT2B7.	119
3.57	Cornish-Bowden plots of the inhibitory effect of andrographolide on the formation rate of (A) morphine-3-glucuronide and morphine-6-glucuronide in recombinant UGT2B7.	120
3.58	Dixon plots of the inhibitory effect of <i>Curcuma xanthorrhiza</i> ethanolic extract on the formation rate of (A) morphine-glucuronide and (B) morphine-6-glucuronide in recombinant UGT2B7.	121

3.59	Cornish-Bowden plots of the inhibitory effect of <i>Curcuma xanthorrhiza</i> ethanolic extract on the formation rate of (A) morphine-glucuronide and (B) morphine-6-glucuronide in recombinant UGT2B7.	122
3.60	Dixon plots of the inhibitory effect of xanthorrhizol on the formation rate of (A) morphine-glucuronide and (B) morphine-6-glucuronide in recombinant UGT2B7.	123
3.61	Cornish-Bowden plots of the inhibitory effect of xanthorrhizol on the formation rate of (A) morphine-glucuronide and (B) morphine-6-glucuronide in recombinant UGT2B7.	124
3.62	Dixon plots of the inhibitory effect of <i>Andrographis paniculata</i> ethanolic extract on the formation rate of (A) morphine-3-glucuronide and (B) morphine-6-glucuronide in human liver microsomes.	125
3.63	Cornish-Bowden plots of the inhibitory effect of <i>Andrographis paniculata</i> ethanolic extract on the formation rate of (A) morphine-3-glucuronide and (B) morphine-6-glucuronide in human liver microsomes.	126
3.64	Dixon plots of the inhibitory effect of andrographolide on the formation rate of (A) morphine-3-glucuronide and (B) morphine-6-glucuronide in human liver microsomes.	127
3.65	Cornish-Bowden plots of the inhibitory effect of andrographolide on the formation rate of (A) morphine-3-glucuronide and (B) morphine-6-glucuronide in human liver microsomes.	128
3.66	Dixon plots of the inhibitory effect of <i>Curcuma xanthorrhiza</i> ethanolic extract on the formation rate of (A) morphine-3-glucuronide and (B) morphine-6-glucuronide in human liver microsomes.	129
3.67	Cornish-Bowden plots of the inhibitory effect of <i>Curcuma xanthorrhiza</i> ethanolic extract on the formation rate of (A) morphine-3-glucuronide and (B) morphine-6-glucuronide in human liver microsomes.	130

- 3.68** Dixon plots of the inhibitory effect of xanthorrhizol on the formation rate of (A) morphine-3-glucuronide and (B) morphine-6-glucuronide in human liver microsomes. **131**
- 3.69** Cornish-Bowden plots of the inhibitory effect of xanthorrhizol on the formation rate of (A) morphine-3-glucuronide and (B) morphine-6-glucuronide in human liver microsomes. **132**

LIST OF SYMBOLS AND ABBREVIATIONS

MOR	: Morphine
M3G	: Morphine-3-glucuronide
M6G	: Morphine-6-glucuronide
KET	: Ketamine
AND	: Andrographolide
NEO	: Neoandrographolide
CUR	: Curcumin
XNT	: Xanthorrhizol
APEE	: <i>Andrographis paniculata</i> Ethanolic Extract
APAE	: <i>Andrographis paniculata</i> Aqueous Extract
CXEE	: <i>Curcuma xanthorrhiza</i> Ethanolic Extract
CXAE	: <i>Curcuma xanthorrhiza</i> Aqueous Extract
UGT	: Uridine 5'-diphospho-glucuronosyltransferase
DME	: Drug Metabolizing Enzyme
IC ₅₀	: Half-Maximal Inhibitory Concentration
V _{max}	: Maximal Reaction Velocity
K _m	: Michaelis-Menten Constant
K _i	: Inhibition Constant
K _i _c	: Competitive Inhibition Constant
K _i _u	: Uncompetitive Inhibition Constant
K _a	: Binding Constant
AUC	: Area Under The Curve
CL _{int}	: Intrinsic Clearance
ICH	: International Conference on Harmonization of Technical Requirement for Registration of Pharmaceutical for Human Use

HPLC	: High-Performance Liquid Chromatography
MPE	: Mean Percentage Error
RSD	: Relative Standard Deviation
QC	: Quality Control
LQC	: Low Quality Control
MQC	: Medium Quality Control
HQC	: High Quality Control
LOD	: Limit of Detection
LOQ	: Limit of Quantification
RCF	: Relative Centrifugal Factor
WHO	: World Health Organization
FDA	: United State of Food and Drug Administration
EMA	: European Medicines Agency
DSHEA	: Dietary Supplement Health and Education Act 1994
BSA	: Bovine Serum Albumin
cDNA	: Complementary DNA
e.g.	: Exempli Gratia (For Example)
i.e.	: Id Est (That is)

EKSTRAK DAN SEBATIAN AKTIF
ANDROGRAPHIS PANICULATA* DAN *CURCUMA XANTHORRHIZA
MERENCAT GLUKURONIDASI MORFINA

ABSTRAK

Baru-baru ini, fenomena interaksi herba-drug telah mendapat perhatian hampir seantero dunia atas sebab tersebarnya populariti penggunaan produk herba dalam bentuk suplemen tambahan. Dalam kajian ini kesan perencatan herba Malaysia yang telah disenaraikan iaitu: hempedu bumi (*Andrographis paniculata*) dan temulawak (*Curcuma xanthorrhiza*) terhadap proses glukuronidasi morfina akan diuji menggunakan model protein rekombinan UGT2B7 dan mikrosom hepar bersumberkan dari manusia. Kesemua ekstrak etanol dan akueus bagi herba hempedu bumi serta andrografolida telah merencatkan aktiviti glukuronidasi morfina kecuali neoandrografolida. Ekstrak akueus merencatkan glukuronidasi morfina secara sederhana jika dibandingkan dengan ekstrak etanol dan andrografolida. Andrografolida adalah fito-konstituen yang dipercayai telah menyumbang besar terhadap trend perencatan yang ditunjukkan oleh ekstrak etanol dan analisis kinetik menunjukkan bahawa kedua-dua ekstrak etanol dan andrografolida merencatkan proses glukuronidasi morfina secara kompetitif (bukan tulen) dengan julat pemalar-perencatan, K_i dari 3.22 hingga 17.94 $\mu\text{g/mL}$ bagi ekstrak etanol dan juga dari 1.35 hingga 15.06 μM bagi andrografolida yang mana kesemuanya dikaji di dalam protein rekombinan dan mikrosom hepar. Sementara itu, ekstrak akueus temulawak didapati tidak mampu merencatkan proses glukuronidasi morfina sekuat ekstrak etanol. Kurkumin pula tidak memberikan sebarang kesan terhadap glukuronidasi morfina manakala xantorhizol merencatkan proses glukuronidasi morfina secara sederhana dalam model protein rekombinan dan mikrosom hepar. Analisis kinetik terhadap xantorhizol menunjukkan bahawa fito-konstituen ini merencatkan glukuronidasi morfina secara kompetitif (sebahagiannya kompetitif tulen dan selebih nya kompetitif bukan tulen) dengan julat pemalar-perencatan, K_i dari 1.07 hingga

116.74 μM manakala ekstrak etanol merencatkan proses glukuronidasi morfina melalui beberapa laluan mekanisme (kompetitif tulen, kompetitif bukan tulen dan bukan kompetitif) dengan julat pemalar-perencatan, K_i dari 3.22 hingga 14.30 $\mu\text{g}/\text{mL}$ dalam model protein rekombinan dan mikrosom hepar. Maklumat dari kajian ini dipercayai dapat menyumbangkan informasi tambahan terhadap mana-mana para penyelidik yang ingin meneruskan kajian ini ke tahap klinikal dan juga ahli-ahli pengamal perubatan yang sering kali berhadapan terhadap pesakit yang dibekalkan dengan preskripsi morfina.

ANDROGRAPHIS PANICULATA AND CURCUMA XANTHORRHIZA
EXTRACTS AND ACTIVE CONSTITUENTS INHIBIT
MORPHINE GLUCURONIDATION

ABSTRACT

A resurgence in the widespread popularity of herbal product in its supplement forms has recently attracted global attention concerning to herb-drug interaction. The inhibitory effects of selected Malaysian medicinal plant herbs namely *Andrographis paniculata* and *Curcuma xanthorrhiza* on morphine glucuronidation were evaluated on recombinant UGT2B7 protein and human liver microsomes. Ethanolic and aqueous extracts of *Andrographis paniculata* as well as andrographolide inhibited morphine glucuronidation at various degrees except for neoandrographolide. Aqueous extract moderately inhibited morphine glucuronidation compared to andrographolide and ethanolic extract. Andrographolide is the main perpetrator that contributes to the potent inhibitory action of ethanolic extract and kinetic analysis has suggested that andrographolide and *Andrographis paniculata* ethanolic extract competitively (mixed competitive) inhibited morphine glucuronidation featuring competitive inhibition constant, K_{i_c} values ranging from 1.35 to 15.06 μM for andrographolide and 3.22 to 17.94 $\mu\text{g/mL}$ for *Andrographis paniculata* ethanolic extract on both recombinant UGT2B7 protein and human liver microsomes. Meanwhile, ethanolic extract of *Curcuma xanthorrhiza* strongly inhibited morphine glucuronidation while that of aqueous extract had displayed moderate inhibition trend on both recombinant UGT2B7 protein and human liver microsomes. Xanthorrhizol inhibited morphine metabolism not as potent as ethanolic extract whereas curcumin did not pose any significant inhibitory trend on morphine glucuronidation. Kinetic assessment has shown that xanthorrhizol competitively (pure and mixed competitive) inhibited morphine glucuronidation with K_{i_c} values ranging from 1.07 to 116.74 μM whereby *Curcuma xanthorrhiza* ethanolic extract inhibited morphine glucuronidation through various modes of

inhibition (pure competitive, mixed competitive and non-competitive) with K_{i_c} values ranging from 3.22 up to 14.30 $\mu\text{g/mL}$ on both recombinant UGT2B7 protein and human liver microsomes. Data generated from this study is expected to provide supplementary information particularly for researchers with intention to conduct clinical study in humans and for the clinicians who routinely deal with patients that are prescribed with morphine.

CHAPTER 1

INTRODUCTION

1.1 Background and Highlights

The use of herbal medicines to treat ailments has been part of mankind's attempt to escape from sicknesses for millennia. As science ascended after the 17th century, the arcane natures of herbal medicines were progressively demystified. Isolation of bioactive chemical species from these herbs became popular and since then, the practice of medicines derived from plant sources have become common in many clinical settings even until today (Solecki 1975).

However, the 1990's had witnessed an outbreak on the market sales of herbal medicines in 'supplement' form which can simply be obtained anywhere or by anyone (Bernard 2005). The word 'supplement' can be interpreted as a blanket term used to promote the practice of alternative medicine through their 'all-natural' claim. This marketing tactic masks the fact that these natural supplements are actually a hotchpotch of potentially biological active compounds that present in the supplement's capsule in unknown quantities. What is worst, these supplements flooded the market and are produced without proper scrutiny from relevant authorities.

On the other hand, it is an undeniable fact that most people nowadays chose to prescribe conventional drugs (e.g. paracetamol) even for treating a headache. When the prescription of conventional drugs combine with the spate of herbal supplement consumptions, the possibility of overlapping between the two will exist. This condition is known as herb-drug interaction and can occur to numerous combinations between herbs and conventional drugs which result to the alteration of drug efficacies that may lead to overdosing or underdosing of the prescribed drug.

This has come to a realization where scientific investigations need to be carried out concerning to the effects of herbal supplements on metabolic process of conventional drugs. In the last decade, interests in studying the involvement of drug metabolizing enzymes on metabolic interaction between herbal supplement and conventional drugs have grown significantly. The number of publications citing herb-drug interactions have increased by nearly five-fold in the 2000's compared to 1990's (Mohamed 2010).

Cytochrome P450 and UGT enzymes are reputed to be the most important species of drug metabolizing enzymes where they are responsible for the clearance of more than 90% of pharmaceutical drugs in the body (Rowland et al. 2013). Several case studies, reports and review articles have documented the potential of herbal products to modulate the activity of cytochrome P450 enzymes (Breidenbach et al. 2000, Haller and Benowitz 2000, Skalli et al. 2007, Izzo and Ernst 2009). On the other hand, similar effects on UGT enzymes have not been sufficiently studied (Mohamed and Frye 2011a).

A number of findings have investigated the effect of selected herbal medicines on UGT enzymes activities (Abidin 2014, Salleh 2014). Each study examined different herbal plants (*Andrographis paniculata* and *Curcuma xanthorrhiza*) on their inhibitory effects on UGT enzymes activities. A concept has been built based on the conclusions of both projects which stated: *Andrographis paniculata* and *Curcuma xanthorrhiza* will inhibit the metabolism of drugs that are primarily metabolized by UGT2B7 – one of the sub-family of UGT enzyme (Coffman et al. 1997).

This study attempts to prove the proposed concept of previous findings by assessing the metabolic activity of morphine which primarily metabolized by UGT2B7 to be inhibited by *Andrographis paniculata* or *Curcuma xanthorrhiza* in human *in-vitro* enzyme system. As morphine does not follow any metabolic pathway in human except for glucuronidation by UGT2B7, herb-drug interaction between studied plant herbs and morphine is hypothetically

to occur. Evaluation through *in-vitro* inhibition assay using appropriate kinetic model is necessary to predict the potentiality of both herbal plants to inhibit the metabolism of morphine in human.

Data generated from this study will provide useful information especially for researchers with intention to conduct further clinical study in human and for the clinicians that routinely deal with patients that are prescribed with morphine to always stay in precaution pertinent to morphine interaction side effects.

1.2 Herbal Medicines

1.2.1 Medicinal Plant Herbs

Plants have played a vital role in maintaining human health and improving their quality of life for many centuries. In botanology, herbs refer to seed-producing plant with non-woody stem that die at the end of growing season whereas, in the field of herbal medicine, the term herb is used loosely to refer not only to seed-producing plant, but also appointed to any parts of plant such as fruits, seeds, roots, leaves, flowers and barks that display medicinal properties. Herbal plants are commonly used in primary form or occasionally combined into mixtures. Pharmacologically active phytoconstituents such as polyphenols, alkaloids, flavonoids, terpenoids, anthraquinones, coumarins, saponin, or tannins may present in herbal plants. Those constituents are considered to be very useful due to their various biological activities including anti-oxidant, anti-inflammatory or anti-cancer properties (Zhou et al. 2007).

Today, under the bill of Dietary Supplement Health and Education Act 1994 (DSHEA), herbs belong to a class of dietary supplement which severely limits the US Food and Drug Administration's (FDA) ability to regulate this class of substances. Unlike pharmaceutical drug, medicinal herbs under the bill of DSHEA requires no proof of efficacy, no proof of safety, and sets no standards for quality control for any product to be labelled as a dietary supplement. Since then, productions of herbal supplements by the industries have become viral (Bauer 2003). It is estimated that the global market for herbal products to be worth around US\$80 to US\$100 billion representing an annual growth rate ranging from 5% to 15% (Gohil and Patel 2007).

In Malaysia, herbal products form the largest group of registered medicines (37.1%), compared with prescription drugs (32.2%) and over-the-counter (non-prescription) drugs (23.9%) (Ang 2005). From 2000 to 2005, annual sales for herbal products in Malaysia increased from US\$0.385 to US\$1.29 billion (Aziz and Tey 2009). The government has

highlighted several core strategies to turn Malaysia into a high income economy by the year of 2020. This has led to the introduction of the 12 National Key Economic Areas (NKEA) which includes agriculture as one of the main important keys. Under the nation's agriculture NKEA, sixteen entry point project (EPP) have been identified with herbal product ranked as the first out of sixteen. In the beginning, five herbal plants namely, *Eurycoma longifolia* (tongkat ali), *Orthosiphon stamineus* (misai kucing), *Andrographis paniculata* (hempedu bumi), *Gynura procumbens* (dukung anak) and *Labisia pumila* (kacip fatimah) were listed as the high-value herbal products. Five R&D clusters were established which focus on discovery, processing technology, crop production, product standardization and pre-clinical/clinical studies to further support the EPPs. Initially, the project aimed of producing high-value herbal products totalling RM 2.2 billion of the Gross National Income (GNI) along with the proposed five herbal plants. At present six more herbal plants have been added to the project including *Morinda citrifolia* (mengkudu), *Hibiscus sabdariffa* (roselle), *Zingiber officinale* (ginger), *Ficus deltoidea* (mas cotek), *Clinacanthus nutans* (belalai gajah) and *Centella asiatica* (pegaga). The market potential of all eleven herbs are being studied at current and developed under the 10th Malaysian Plan. With increasing market demand globally and locally, there is a need for rigorous scientific examination of herbal medicines as it may lead to greater acceptance by mainstream practitioners.

1.2.2 *Andrographis paniculata*

Andrographis paniculata is an erect annual herb, growing to a height of 30 to 90 cm. The leaves are sessile, dark green in colour, glabrous and are lanceolate in shape. The aerial part of the plant, including leaves and stems are frequently used as traditional medicine. Morphology of the plant parts are shown below (**Figure 1.1**):

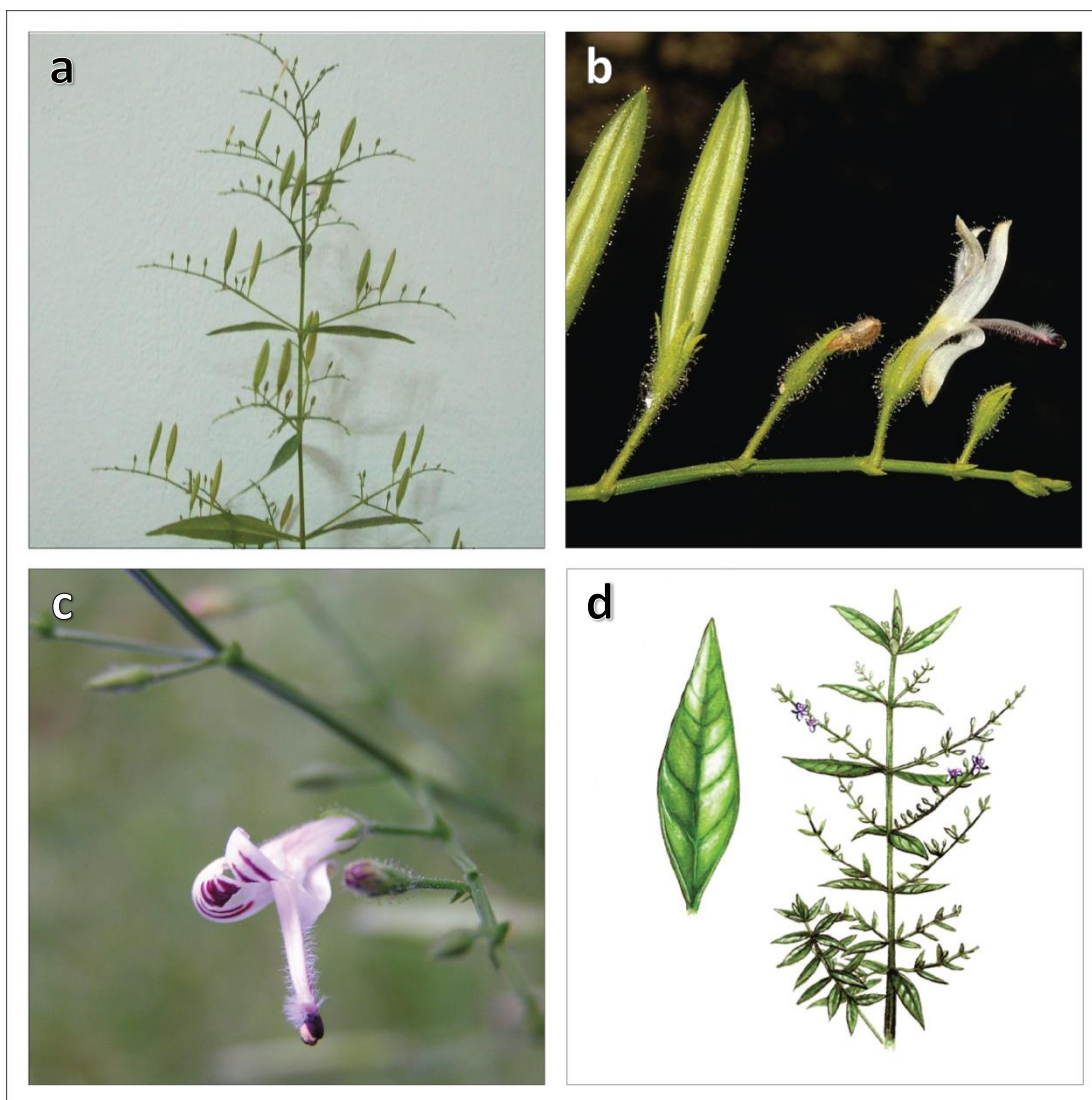


Figure 1.1 Morphology of *Andrographis paniculata* plant parts. (a) Herb in pod stage with terminal and axillary panicles, (b) flowering plant with a small opened flower, (c) a flower with opened anther and pollen grains, (d) schematic drawing of *Andrographis paniculata*.

1.2.2 (a) Taxonomic Hierarchy

Kingdom	:	Plantae
Subkingdom	:	Viridiplantae
Infrakingdom	:	Streptophyta
Superdivision	:	Embryophyta
Division	:	Tracheophyta
Subdivision	:	Spermatophytina
Class	:	Magnoliopsida
Superorder	:	Asteranae
Order	:	Lamiales
Family	:	Acanthaceae
Genus	:	<i>Andrographis</i>
Species	:	<i>Andrographis paniculata</i> (Burm. f.) Wall. ex Nees

1.2.2 (b) Phytochemistry of *Andrographis paniculata*

Phytochemical analysis of this plant has revealed a myriad species of diterpenoids, flavonoids and phytophenols. Diterpenoids are the major phytoconstituents of *Andrographis paniculata* which can be isolated in free and glycoside form. A number of chemical species which have been reported includes: andrographolide, andrographiside, neoandrographolide, 6'-acetylneoandrographiside, 14-deoxy-11,12-didehydroandrographolide, 14-deoxy-11,12-didehydroandrographiside, 14-deoxyandrographolide, 14-deoxyandrographiside, andrographanin, andropanoside, isoandrographolide, andrographatoside, andropanolide, 5-hydroxy-7,8,2'-trimethoxyflavone, 5,2'-dihydroxy-7,8-dimethoxyflavone, 5-dihydroxy-7,8-dimethoxyflavone, 5-dihydroxy-7,8-dimethoxyflavanone and andrographidine (Kleipool 1952, Chan et al. 1971, Balmain and Connolly 1973, Smith et al. 1982, Rao et al. 2004, Pramanick et al. 2006, Shen et al. 2006, Xu et al. 2010, Lim et al. 2012).

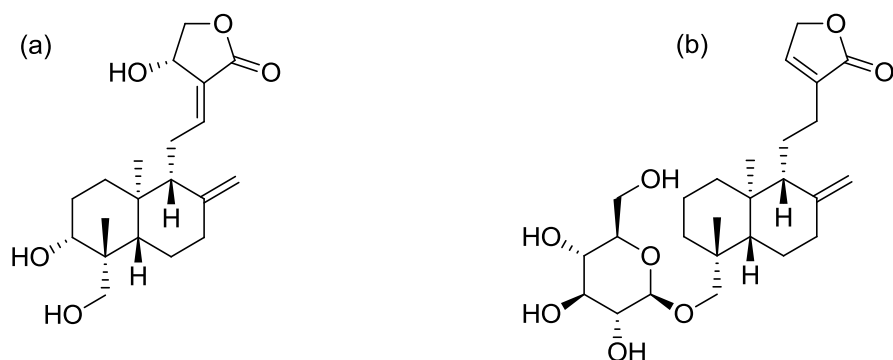


Figure 1.2 Selected phytoconstituents of *Andrographis paniculata* to be used in the study: (a) andrographolide and (b) neoandrographolide.

1.2.2 (c) Pharmacological Properties of *Andrographis paniculata*

Various reports have documented various biological activities and therapeutic value of *Andrographis paniculata* and its active phytoconstituents. It includes hepatoprotective, hypoglycaemic, cardioprotective, anti-inflammatory, immunostimulatory, anti-cancer, anti-HIV as well as antimalarial properties (Jarukamjorn and Nemoto 2008, Chao and Lin 2010, Akbar 2011).

Despite the usefulness and widespread use, information concerning the potential of this plant on drug metabolizing enzymes is quite limited. The growing awareness of herb-drug interaction has led to a number of studies on the modulatory effect of *Andrographis paniculata* or its phytoconstituents on cytochrome P450 enzyme activity, the so-called main drug metabolizing enzymes (Pekthong et al. 2009, Pan, Rashid, et al. 2011, Tan and Lim 2014). However, the potential of herb-drug interaction on other metabolic pathways beside cytochrome P450 still exist and should be given a proper attention.

1.2.3 *Curcuma xanthorrhiza*

Curcuma xanthorrhiza is a perennial herbaceous plant, growing to a height of 1 m tall. Commonly known as Javanese turmeric or temulawak, this herb is one of the family members of ginger which originated from Indonesia. It can also be found in Malaysia, Sri Lanka, Thailand and Philippines. It is highly branched with alternate leaves arranged in two rows. The non-aerial part is made up of yellowish tuberous rhizomes (**Figure 1.3**):

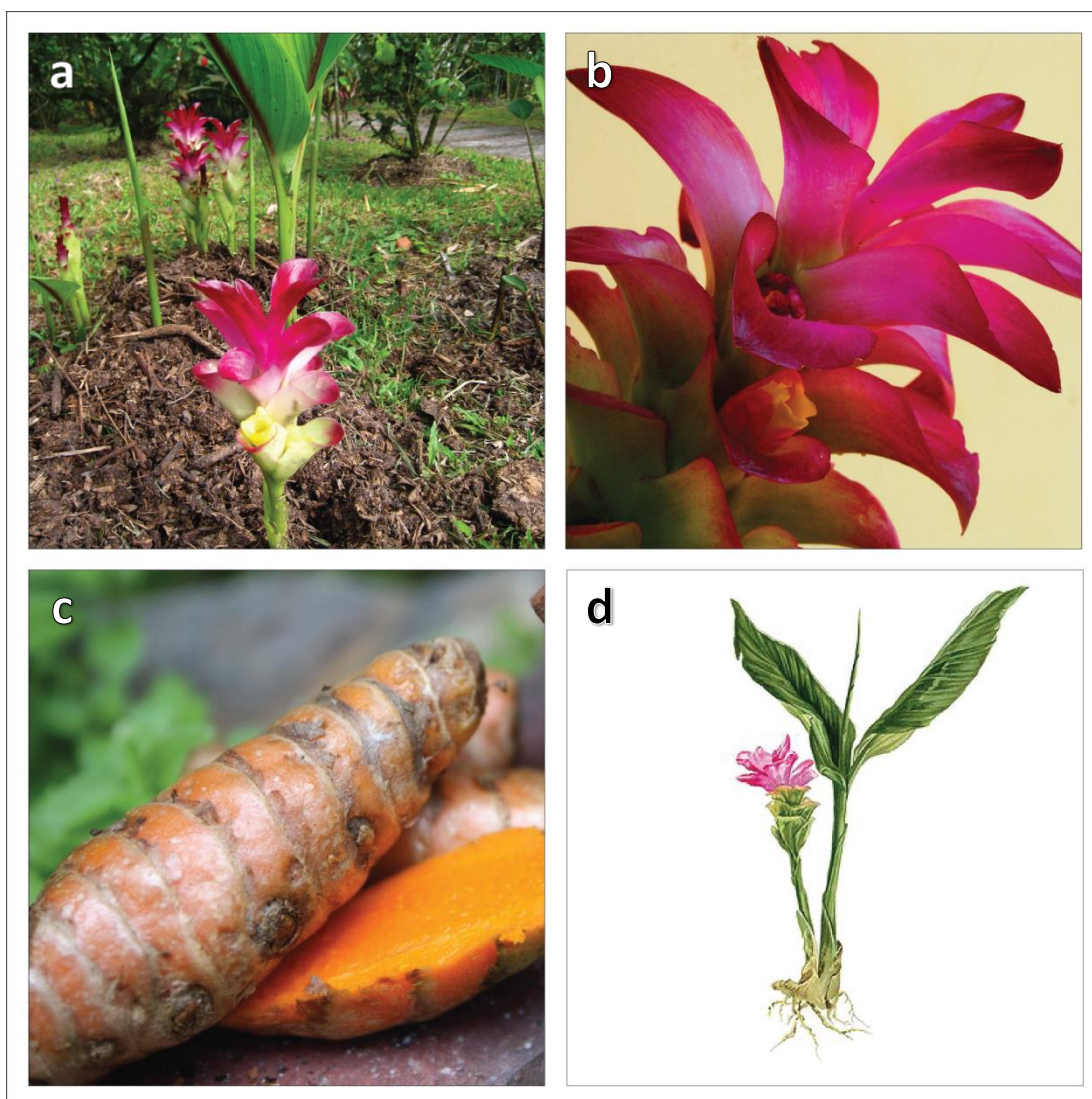


Figure 1.3 Morphology of *Curcuma xanthorrhiza* plant parts. (a) aerial portion of the plant, (b) threefold hermaphrodite flowers, (c) yellowish-orange cylindrical rhizomes, (d) schematic drawing of *Curcuma xanthorrhiza*.

1.2.3 (a) Taxonomic Hierarchy

Kingdom	:	Plantae
Subkingdom	:	Viridiplantae
Infrakingdom	:	Streptophyta
Superdivision	:	Embryophyta
Division	:	Tracheophyta
Subdivision	:	Spermatophytina
Class	:	Magnoliopsida
Superorder	:	Lilianae
Order	:	Zingiberales
Family	:	Zingiberaceae
Genus	:	Curcuma
Species	:	<i>Curcuma xanthorrhiza</i> Roxb.

1.2.3 (b) Phytochemistry of *Curcuma xanthorrhiza*

Investigation of phytochemical content of this plant has shown that *Curcuma xanthorrhiza* contains various classes of phytochemicals. It includes curcuminoids (mixture of curcumin, monodemethoxycurcumin, bis-demethoxycurcumin), sesquiterpenes (β -curcumene, ar-curcumene, bisabolane, lactone germacrone), flavonoids (catechin, epicatechin, quercetin, myricetin, kaempferol, apigenin, luteolin, naringenin), camphor and xanthorrhizol (Zwaving and Bos 1992, Jarikasem et al. 2003, Ruslay et al. 2007, Tsai et al. 2011, Jantan et al. 2012).

Evaluation of the presence of xanthorrhizol and the absence of bisdemethoxycurcumin are the best ways to distinguish between *Curcuma xanthorrhiza* (Javanese turmeric) and *Curcuma longa* (turmeric) (Jantan et al. 2012).

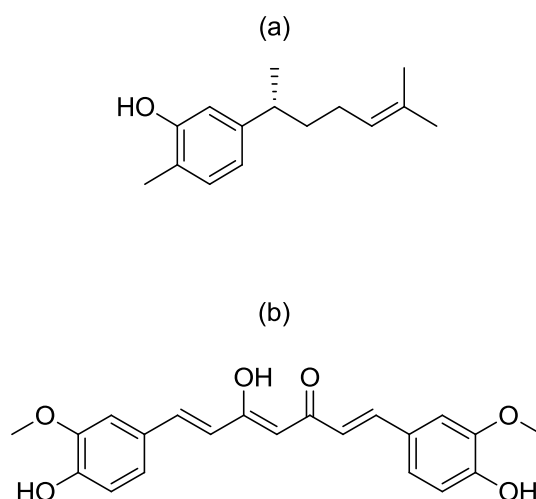


Figure 1.4 Selected phytoconstituents of *Curcuma xanthorrhiza* to be used in the study: (a) xanthorrhizol and (b) curcumin.

1.2.3 (c) Pharmacological Properties of *Curcuma xanthorrhiza*

The rhizomes of this plant have been traditionally used to treat various diseases including liver disorder, gallstone, jaundice and to promote the flow of biliary secretion. Apart from medicinal purposes, *Curcuma xanthorrhiza* is also commonly used in food making (Ismail et al. 2005, Cheah et al. 2006, Hatcher et al. 2008, Cheah et al. 2009, Kang et al. 2009, Kim et al. 2012).

The principal components of *Curcuma xanthorrhiza* are xanthorrhizol and curcumin. The two components possess a wide range of pharmacodynamic values which have been shown capable to overlap to produce synergistic therapeutic effect (Cheah et al. 2009). Curcumin also is one of the main constituent of *Curcuma longa*. For that reason, it had undergoes various pharmacokinetic study where it has been shown that curcumin demonstrates poor systemic bioavailability due to rapid metabolism in the gut and liver (Vareed et al. 2008). Unlike curcumin, xanthorrhizol having much less attention concerning to its pharmacokinetic nature. At present, there are no bioavailability data of xanthorrhizol as well as information on its metabolic pathway particularly in mammals.

1.3 Drug Metabolism

Drug metabolism is a biochemical reaction of pharmaceutical substances catalyzed by a group of specialized enzymes, notable to many as drug metabolizing enzymes. It covers three phases in which phase I involves the redox (reduction and oxidation) reaction of the substances while Phase II performs chemical conjugation process and phase III is the involvement of membrane transporter on the excretion of drugs and their metabolites (Changjiang et al. 2005).

1.3.1 Drug Metabolizing Enzymes

Drug metabolizing enzymes are diverse classes of proteins that are responsible for metabolizing a myriad species of pharmaceutical substances. Metabolic biotransformation of drugs by these enzymes forms a more hydrophilic metabolite which not only leads to the deactivation of the pharmacologically active drugs but also enhancing the excretion process in the body. As a result, the functional homeostasis of the cell is preserved in the face of chemical challenges (Penner et al. 2012).

Phase I drug metabolizing enzymes catalyze the modification of chemical functional groups within a molecule to improve its hydrophilicity. Such reactions are catalyzed by a number of protein enzymes which include cytochrome P450s, aldehyde oxidases, monoamine oxidases and flavin-containing monooxygenases (Iyanagi 2007).

Phase II drug metabolizing enzymes carry out chemical conjugation process where it involved the transfer of a hydrophilic moiety entity onto a substrate which greatly enhance its water solubility nature as compared to phase I. Phase II biotransformation reactions include sulfonation, glucuronidation or glutathione conjugation. Enzymes that involved in phase II stage are the sulfotransferases, Uridine 5'-diphospho-glucuronosyl transferases and glutathione S-transferases (Petra and Michal 2012).

1.3.2 UGT Enzymes

Uridine 5'-diphospho-glucuronosyltransferases (UGTs) are superfamily of protein enzymes that are responsible for metabolism of endobiotics and xenobiotics in many organisms including humans. UGT enzymes play a major role in catalyzing a conjugation process known as glucuronidation. During glucuronidation, a glucose-derived moiety, glucuronic acid is conjugated to a suitable functional site (hydroxyl, carboxyl, carbonyl, sulfhydryl, and amine) on a substrate modulated by UGT proteins (**Figure 1.5**). Generally, this metabolic process generates a highly soluble inactive metabolite which renders excretion process in the body.

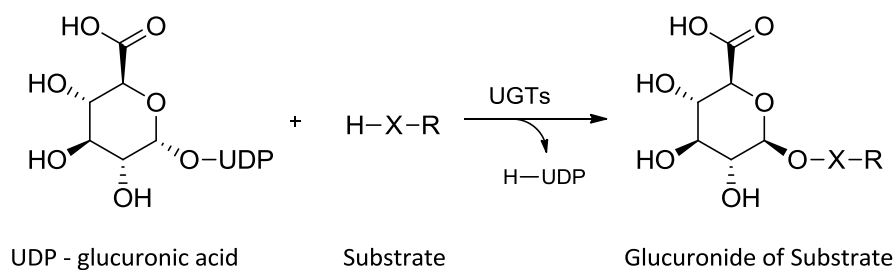


Figure 1.5 Glucuronic acid conjugation of a substrate catalyzed by UGT enzymes producing a highly soluble metabolite.

UGT enzymes display a broad and overlapping substrate specificities, which are common features for drug-metabolizing enzymes (Court et al. 2005). Human UGTs are divided into two families, UGT1 (1A1, 1A3, 1A4, 1A5, 1A6, 1A7, 1A8, 1A9, 1A10) and UGT2 (2A1, 2A3, 2B4, 2B7, 2B10, 2B11, 2B15, 2B28). These two families originated from two separated genes located on chromosome 2q37 and 4q13 which encode a number of different proteins yet, still perform the same glucuronidation function (Mackenzie et al. 2005). Inhibition of UGT metabolic activities may cause serious threats especially in metabolizing environmental toxicants or native endobiotics for example bilirubin, a by-product of haemoglobin catabolism which can only be removed via conjugation with glucuronic acid (Desai et al. 2003).

1.3.3 Latency of Microsomal UGTs

UGT proteins are believed to be localized within the luminal wall of endoplasmic reticulum (Figure 1.6).

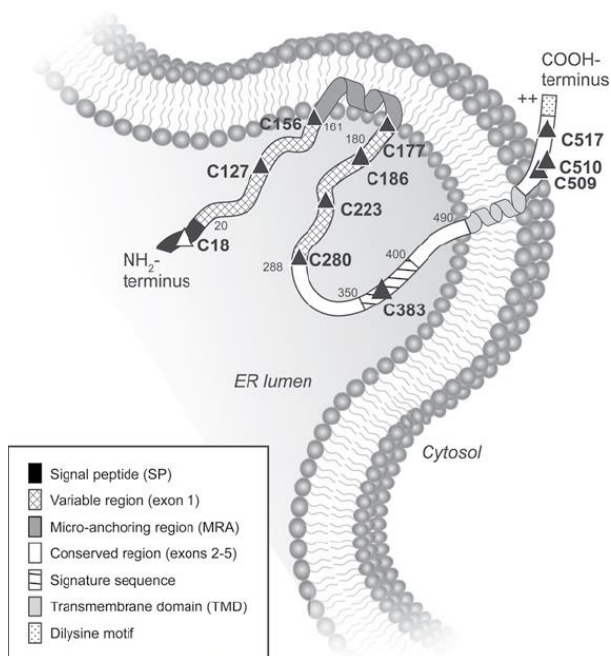


Figure 1.6 Schematic representation of UGT protein (UGT1A1) within the luminal wall of endoplasmic reticulum (ER). Almost the entire polypeptide chain resides in the lumen, except for the COOH-terminus. (Rouleau et al. 2013).

It has been suggested that the existence of active transporters in living system is vital in order to translocate the substrate from cytosolic space into the lumen where UGT active site is located. Without active transporter, glucuronidation reaction will become latent and slower than it should be. The latency seen in microsomal glucuronidation is thought to be due to the presence of a membrane obstructing the free access of substrate to the enzyme. Fully functional transporters are assumed to exist in hepatocytes but optimal microsomal glucuronidation requires an activation step which disrupts the membrane thereby permitting the flow of substrate between the cytosol and the lumen (Ishii et al. 2012). Several treatments activate the microsomal glucuronidation reaction particularly detergents, physical disruption, sonication and the pore-forming agent alamethicin. In absence of activation, microsomal

UGT remains in a latent state. Incubation of microsomal UGT with alamethicin activates the microsomal glucuronidation activity by 10 folds higher compared to the untreated microsomes. It was discovered that alamethicin embedded itself in cluster on the endoplasmic reticulum membrane to form a well-define pore (**Figure 1.7**). The microsomal glucuronidation is also stimulated by Mg^{2+} and hence incubation are routinely supplemented with $MgCl_2$ (Pang et al. 2009).

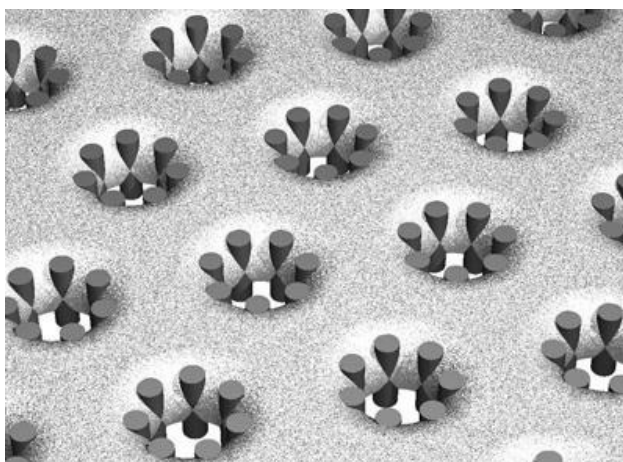


Figure 1.7 Schematic of alamethicin pores in membrane bilayer. Each pore comprises eight units of alamethicin align in barrel-stave fashion. (He et al. 1995).

1.3.4 *In-vitro* Model

Since liver plays a major role in drug metabolism, there are many models that have been built to imitate the organ's metabolic process. There are various *in-vitro* tools in studying drug metabolism where this study has decided to focus on two models that commonly used by researchers around the world; the recombinant expressed protein and human liver microsomes.

Human drug metabolizing enzymes have been genetically engineered from various recombinant expression systems including bacteria, insect or other mammalian cell systems. The isolated protein of the expression system provides an important functional assay for

single protein species worth for the study of various fields of drug metabolism (Plant 2004). The baculovirus-insect cell expression system is the most common recombinant model used today due to its absence or lack of cytochrome P450 and UGT protein species. Taking advantage of that characteristic, the insect cells can be transfected with cDNA of human UGTs to express desired protein species. The major benefit of this model is its simplicity and allowing the study of specific enzyme separately. The major drawback of recombinant protein is the difference in the metabolic activity of enzyme per unit of microsomal protein compared to that in human liver microsomes (Baranczewski et al. 2006).

Human liver microsome is one of the main sources of drug metabolizing enzymes. Microsomes are not ordinarily present in living cell. It is a fraction of cellular debris which is produced in the laboratory through centrifugation technique. Microsomes can be separated out via differential centrifugation. Most organelles will be sediment-out at 10 000g while soluble enzymes and fragmented endoplasmic reticulum remain in the supernatant fraction. At 100 000g, endoplasmic reticulum will be precipitated out leaving soluble enzymes to remain in the solution. The resulting pellet is the microsomal fraction which contain the cytochrome P450 and the UGTs. However, the addition of exogenous co-factors or co-substrate such as NADPH or UDPGA is necessary to activate the enzymes. It is said that, liver microsomes are one of the best characterized *in-vitro* tool for drug metabolism studies beside being low in cost and the ease of handling the system (Brandon et al. 2003).

1.3.5 Drug Interaction through Glucuronidation

Drug Interaction is a condition whereby a substance affects the activity of a drug when both are administered together. Drug interaction often involved the inhibition of drug metabolizing enzyme activity, resulting in increased systemic exposure and subsequent adverse effect. In other cases, induction of drug metabolizing enzyme expression resulted in reduced systemic exposure leading to the risk of loss of efficacy. Like many enzymes, UGTs also have the potential to be inhibited which may affect the glucuronidation of substrates

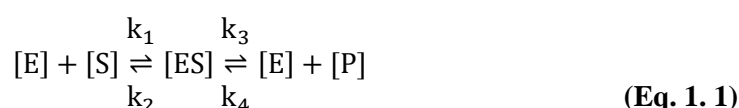
catalyzed by these enzymes. Therefore, there is a potential for consequences that affecting clinical efficacy in UGT-mediated drug interaction. It gets worst when the metabolism of a substance exclusively follows glucuronidation pathway like zidovudine, codeine and morphine which can result in a significant increase of drugs exposure upon inhibition. Similarly important, since many phytochemicals are also substrates for UGTs, herb-drug interactions via glucuronidation pathway is always possible and should not be neglected when studying drug interactions (Mohamed and Frye 2011a).

1.4 Enzyme Kinetics

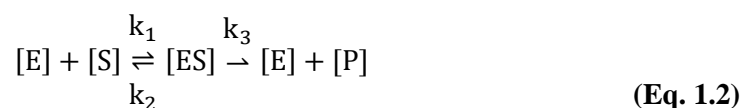
Enzyme kinetics is a way to learn and predict the behaviour of enzymes through mathematical relationship. It has become an important part in ADME (absorption, distribution, metabolism, excretion) studies where estimation of various kinetic parameters such as V_{max} , K_m and K_i are carried out in determining the degree of involvement of a particular enzyme in presence of substrate and inhibitor. This ultimately leads to the extrapolation of data from *in-vitro* to *in-vivo* model to predict the likelihood of a factor to occur in a real system supplemented by laboratory data.

1.4.1 Michaelis-Menten Kinetics

In 1913, German biochemist Leonor Michaelis and Canadian physician Maud Menten have proposed a mathematical relationship between enzyme and its substrate (Michaelis and Menten 1913). It involves a substrate [S] binds to an enzyme [E] forming a transition complex [ES] and later on converted into product [P] and enzyme [E] in reversible fashion:



It was during 1925, an improvement of Michaelis-Menten kinetics was proposed by Briggs and Haldane (1925) where the formation of [P] was assumed to be purely forward reaction and the introduction of quasi-steady state to simplify the equation as shown below:



The quasi-steady state assumes the concentration of enzyme-substrate complex [ES] is unchanged at the early stage of reaction which can be expressed as, $d[ES] = 0$ (**Figure 1.8**).

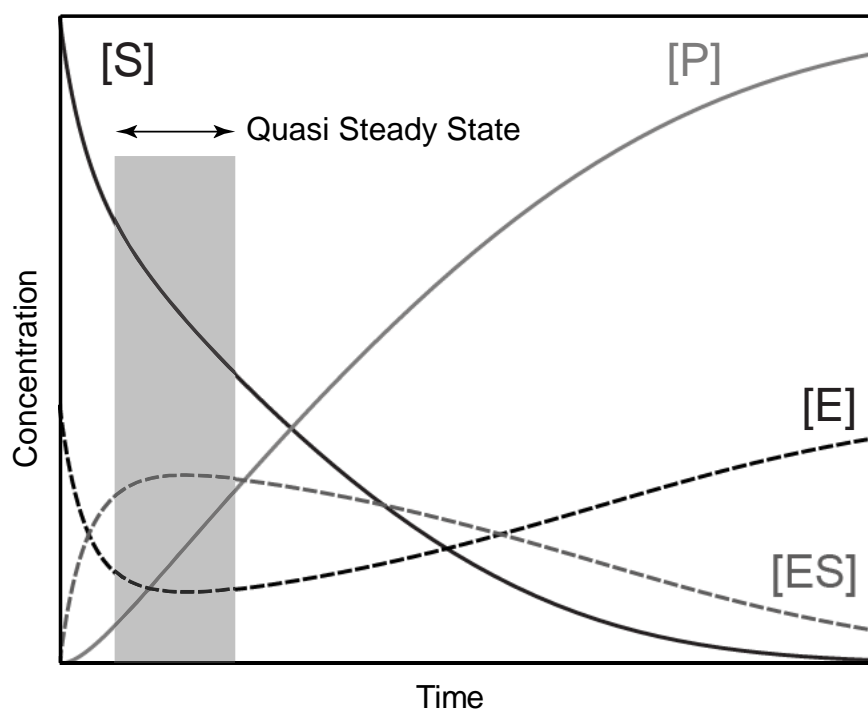


Figure 1.8 Change in concentration over time of enzyme [E], substrate [S], enzyme-substrate complex [ES] and product [P]. The quasi steady state assumes the formation of [ES] to be constant and $d[ES] = 0$ throughout its effect.

From equation (**Eq. 1.2**), a number of rate law equations applying the law of mass action can be proposed as shown below:

$$\frac{d[E]}{dt} = -k_1[E][S] + k_2[ES] + k_3[ES] \quad (\text{Eq. 1.3})$$

$$\frac{d[S]}{dt} = -k_1[E][S] + k_2[ES] \quad (\text{Eq. 1.4})$$

$$\frac{d[P]}{dt} = k_3[ES] \quad (\text{Eq. 1.5})$$

$$\frac{d[ES]}{dt} = k_1[E][S] - k_2[ES] - k_3[ES] \quad (\text{Eq. 1.6})$$

The latter equation (**Eq. 1.6**) describes the rate of change of the [ES] complex. At initial of reaction, [ES] concentration will rapidly approach the quasi-steady state that is after initial burst phase. Its concentration will not change significantly until a significant amount of substrate has been consumed. $d[ES]$ can be assumed as 0 as long as kinetic measurement is carried out under quasi-steady state.

When $d[ES] = 0$,

$$\frac{d[ES]}{dt} = 0 \quad (\text{Eq. 1.7})$$

$$0 = k_1[E][S] - k_2[ES] - k_3[ES] \quad (\text{Eq. 1.8})$$

$$k_1[E][S] = k_2[ES] + k_3[ES] \quad (\text{Eq. 1.9})$$

$$k_1[E][S] = (k_2 + k_3)[ES] \quad (\text{Eq. 1.10})$$

$$[E][S] = \left(\frac{k_2 + k_3}{k_1} \right) [ES] \quad (\text{Eq. 1.11})$$

Michaelis-Menten Constant, $K_m = \frac{k_2+k_3}{k_1}$ therefore,

$$[E][S] = K_m[ES] \quad (\text{Eq. 1.12})$$

Total enzyme concentration $[E]_t$ is the sum between free enzyme $[E]$ and enzyme-substrate complex $[ES]$ where $[E]_t = [E] + [ES]$.

Hence, $[E] = [E]_t - [ES]$

$$([E]_t - [ES])[S] = K_m[ES] \quad (\text{Eq. 1.13})$$

$$[E]_t[S] - [ES][S] = K_m[ES] \quad (\text{Eq. 1.14})$$

$$[E]_t[S] = K_m[ES] + [ES][S] = [ES](K_m + [S]) \quad (\text{Eq. 1.15})$$

$$[ES] = \frac{[E]_t[S]}{K_m + [S]} \quad (\text{Eq. 1.16})$$

Formation rate of product $[P]$ is the measured reaction velocity, $v = \frac{d[P]}{dt} = k_3[ES]$

$$[ES] = \frac{v}{k_3} = \frac{[E]_t[S]}{K_m + [S]} \quad (\text{Eq. 1.17})$$

$$v = \frac{k_3[E]_t[S]}{K_m + [S]} \quad (\text{Eq. 1.18})$$

Since V_{\max} is the reaction velocity during all enzymes is saturated with its substrate $[E]_t$,

$$V_{\max} = k_3[E]_t$$

Therefore,

$$v = \frac{V_{\max} \cdot [S]}{K_m + [S]} \quad (\text{Eq. 1.19})$$

The relationship above is the well-known Michaelis-Menten equation where v is the reaction velocity (rate of product formation), $[S]$ is the substrate concentration, V_{\max} is the maximal velocity of the reaction and K_m is the Michaelis-Menten constant where it represents the ratio of equilibrium constants of $[ES]$ formation (k_1) and its dissociation (k_2 and k_3). K_m also represents the affinity of substrate toward its enzyme as a small K_m value indicates a larger k_1 value which means forward reaction of $[E]+[S]$ is favourable.

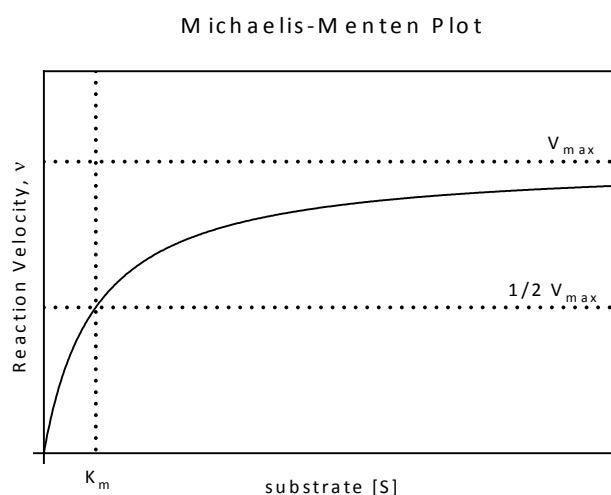


Figure 1.9 Representative hyperbolic plot of a reaction following Michaelis-Menten Kinetics.

A plot of reaction velocity, v as a function of the substrate concentration, $[S]$ as depicted above shows that the maximal velocity V_{\max} is approached asymptotically for an enzyme that obeys Michaelis-Menten kinetics (**Figure 1.9**). This is due to the saturation of enzyme at high substrate concentrations provided the amount of enzyme is fixed during the reaction.

1.4.2 Initial Rate of Reaction

In kinetic studies, it is common practice to perform measurement of reactant(s) and/or product(s) at initial rate as it excludes the contribution of reagents while at excess. In

perspective of Michaelis-Menten Kinetics, the equation assumes no product reversibility (purely forward reaction) and formation of enzyme-substrate complex [ES] occurs at quasi-steady state condition. Both assumptions can be satisfied only if measurements are being made during the stage of initial rate (formation of product less than 10%). Incubation time and protein content are the two parameters that can be optimized to achieve the state of initial rate. It is of little importance to prioritize any of the two as long the formation of product is still less than 10% but both parameters do have several effects to one another especially in terms of speed of reaction. To achieve 10% product formation in short amount of time, a large amount of protein (enzyme) is required which translate to faster catalytic activity whereas small amount of protein will lengthen the time of reaction in order to accomplish the same task.

1.4.3 Linear transformation of Michaelis-Menten Kinetics

Since the relationship between the independent variable v and dependent variable $[S]$ is non-linear, it has long been customary to facilitate estimation of the two variables by linearized the relationship which was first proposed by Lineweaver and Burk (1934):

Taking the reciprocal of both sides of Michaelis-Menten Equation (**Eq. 1.19**),

$$\frac{1}{v} = \frac{K_m + [S]}{V_{\max} \cdot [S]} \quad (\text{Eq. 1.20})$$

$$\frac{1}{v} = \frac{K_m + [S]}{V_{\max} \cdot [S]} = \frac{K_m}{V_{\max} \cdot [S]} + \frac{[S]}{V_{\max} \cdot [S]} = \frac{K_m}{V_{\max}} \cdot \frac{1}{[S]} + \frac{1}{V_{\max}} \quad (\text{Eq. 1.21})$$

Hence, the Lineweaver-Burk derivation,

$$\frac{1}{v} = \left(\frac{K_m}{V_{max}} \right) \cdot \frac{1}{[S]} + \frac{1}{V_{max}} \quad (\text{Eq. 1.22})$$

Lineweaver-Burk plot or double-reciprocal plot (**Figure 1.10**) is widely used as a simple graphical method to determine important terms in enzyme kinetics, such as K_m and V_{max} . The y -intercept of Lineweaver-Burk plot is equivalent to the inverse of V_{max} while the x -intercept represent $-1/K_m$.

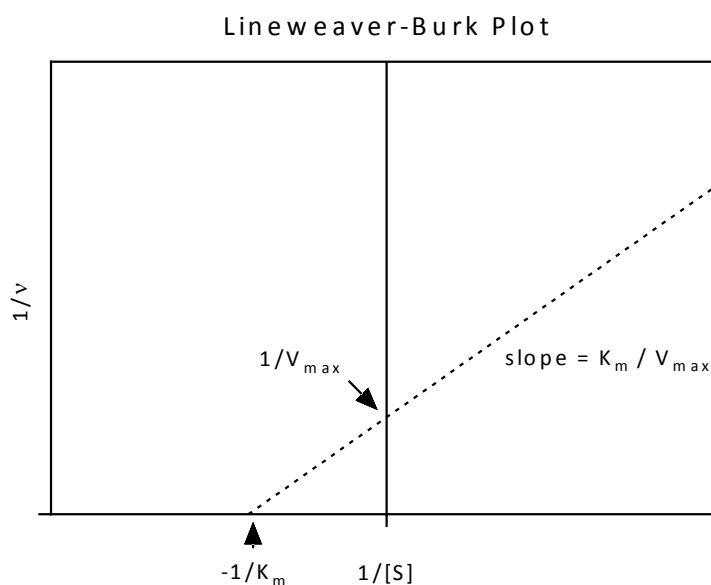
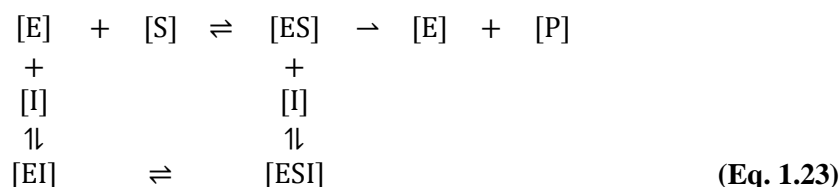


Figure 1.10 Double reciprocal plot of reaction velocity, v as a function of substrate concentration, $[S]$ yielding a linearized Michaelis-Menten relationship.

1.4.4 Enzyme Inhibition

A number of substances may cause a reduction of an enzyme catalytic process causing inhibition. Loss of activity may either be reversible or irreversible. Reversible inhibitor interacts with its target enzyme through simple, reversible binding mechanism where activity may be restored by the removal of inhibitor. Irreversible inhibitor on the other hand deactivates the enzyme where the loss of activity cannot be recovered during the timescale of interest. Heavy metal ions (e.g. lead or mercury) usually cause such irreversible inhibition by binding strongly to the amino acid backbone (Chaplin and Bucke 1990). For most enzyme-

catalyzed processes, the occurrence of reversible inhibition is more common and it is generally discussed in term of a simple expansion of Michaelis-Menten reaction scheme:



Where [I] represents the inhibitor, [EI] represents the enzyme-inhibitor complex and [ESI] represent the enzyme-substrate-inhibitor complex. Reversible inhibitor may be competitive, uncompetitive, mixed or non-competitive depending upon its point of entry into the enzyme.

1.4.4 (a) Competitive-Type Inhibition

Competitive inhibition occurs when both substrate and inhibitor compete for the same active site on the enzyme. Competitive type is most noticeable at low substrate concentration but can be overcome at high substrate concentration as the V_{\max} remains unaffected.

From the expansion of Michaelis-Menten reaction scheme (Eq. 1.23), competitive inhibition will involve additional relationship between enzyme and inhibitor with its respective equilibrium constants:



From (Eq. 1.24), an additional rate law can be proposed,

$$\frac{d[EI]}{dt} = k_4[E][I] - k_5[EI] \tag{Eq. 1.25}$$